

Redox-Active Star Molecules Incorporating the 4-Benzoylpyridinium Cation: Implications for the Charge Transfer Efficiency along Branches vs Across the Perimeter in Dendrimers

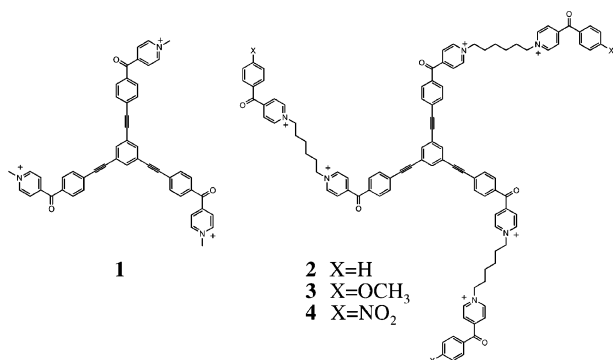
Nicholas Leventis,^{*,†} Jinhua Yang,[‡] Eve F. Fabrizio,[§] Abdel-Monem M. Rawashdeh,[‡] Woon Su Oh,[‡] and Chariklia Sotiriou-Leventis^{*,‡}

NASA Glenn Research Center, 21000 Brookpark Road M.S. 49-1, Cleveland, Ohio 44135, Department of Chemistry, University of Missouri-Rolla, Rolla, Missouri 65409, and Ohio Aerospace Institute, 22800 Cedar Point Road, Cleveland, Ohio 44142

Received October 13, 2003; E-mail: Nicholas.Leventis@nasa.gov; cslevent@umr.edu

Dendrimers are self-repeating globular branched star molecules, whose fractal structure continues to fascinate, challenge, and inspire.¹ Functional dendrimers may incorporate redox centers, and potential applications include antennae molecules for light harvesting, sensors, mediators, and artificial biomolecules. Dendrimers with a redox core show no significant inhibition² but also shielding (by the branches)³ and orientation effects (in asymmetric dendrimers) upon the rate of heterogeneous electron transfer.⁴ Dendrimers with redox centers in the branches are also well-known. Using thin-layer-cell electrochemistry, all 21 tetrathiafulvalenes embedded in the branches of a third-generation dendrimer are electrochemically accessible leading to a 42+ cation.⁵ Using pulse radiolysis, Fox reported fast electron transfer (e-transfer) between peripheral biphenyls (donors) and a core acceptor (a Ru(II)-complex).⁶ On the other hand, Crooks has reported incomplete electrolysis of amido amine dendrimers with a viologen functionalized perimeter,⁷ while Amatore and Abruña using ultrafast voltammetry have reported fast e-transfer, despite the 2-nm separation from one another, among the 64 Ru-complexes in the perimeter of a fourth-generation dendrimer adsorbed on a microelectrode;⁸ the fast charge propagation was attributed to the branch flexibility.

On the basis of those reports, e-transfer across the perimeter of dendrimers should depend on their rigidity, but it is unclear whether it would be more or less efficient than e-transfer along the branches. As these questions have important implications for molecular design, they were investigated with star systems **1–4**, serving as models of first- and second-generation redox dendrimers. Cations



1–4 incorporate 4-benzoyl-*N*-alkylpyridinium (BP),⁹ whose redox potential (a) varies along the branches and (b) remains constant at fixed radius. Our strategy was to measure the number of electrons, n_1 , exchanged between **1** and the electrode at different time-scales,

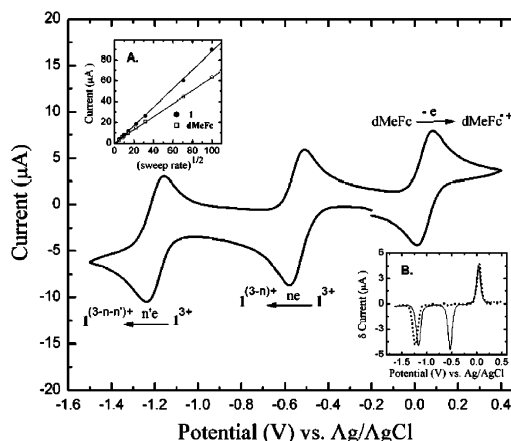


Figure 1. CV at 0.1 V s⁻¹ of **1** (1.10 mM) in Ar-degassed DMF/0.1 M TBAP containing 1.44 mM of dMeFc as internal standard, using a Au disk electrode (1.6 mm in diameter). (Inset A): Same solution Randles–Sevcik plots for **1** and dMeFc in the range 0.02–10 V s⁻¹. For **1**: slope = 0.89 ± 0.01 μA s^{1/2} (mV)^{-1/2}; R² = 0.999. For dMeFc: slope = 0.629 ± 0.003 μA s^{1/2} (mV)^{-1/2}; R² = 1.0. (Inset B): DPV's of **1**/dMeFc (—; 1.02/1.59 mM) and of the free base of **1**-FB/dMeFc (···; 0.98/1.78 mM).

and infer how easily charge randomizes across the perimeter of a relatively small, rigid redox star-system. Thus, n_1 was assessed both at a semi-infinite time scale (by bulk electrolysis) and at the cyclic voltammetric (CV) time scale of 0.02–10 V s⁻¹. Next, the voltammetry of **2–4** was used to assess whether within the same time scale redox centers within the branches are as accessible as redox centers across the perimeter.

Figure 1 shows the redox processes of **1** versus decamethylferrocene (dMeFc: internal standard).¹⁰ One-electron-like waves indicate that redox units behave independently of one another.¹¹ Bulk electrolysis of **1** at -0.85 V vs Ag/AgCl affords $n_1 = 3.01 \pm 0.03$. The linearity of the Randles–Sevcik plot in inset A shows that the number of redox centers reduced remains unchanged in the time scale of 0.02–10 V s⁻¹. Within this time-scale, n_1 was determined first by comparing the ratio of the slopes of the Randles–Sevcik plots of **1** and dMeFc with the limiting current ratio obtained in the same solution with an ultramicroelectrode (~10 μm diam).¹² Thus, $n_1 = 2.08 \pm 0.01$. Alternatively, the diffusion coefficients $D_1 = 9.48 \pm 0.05 \times 10^{-6}$ cm² s⁻¹ and $D_{\text{dMeFc}} = 2.51 \pm 0.03 \times 10^{-5}$ cm² s⁻¹ were determined by an HPLC method (see Supporting Information) and their values were introduced directly in the slope ratio of the Randles–Sevcik plots. Thus, $n_1 = 2.02 \pm 0.07$. The two values of n_1 are comparable. Meanwhile, differential pulse voltammetry (DPV) allows baseline separation of the two reduction waves of **1** (solid line, Figure 1, inset B), and by fitting the nonlinear expression for $(\delta\text{Current})_{\text{max}}$,¹² it is calculated from

[†] NASA Glenn Research Center.[‡] University of Missouri-Rolla.[§] Ohio Aerospace Institute.

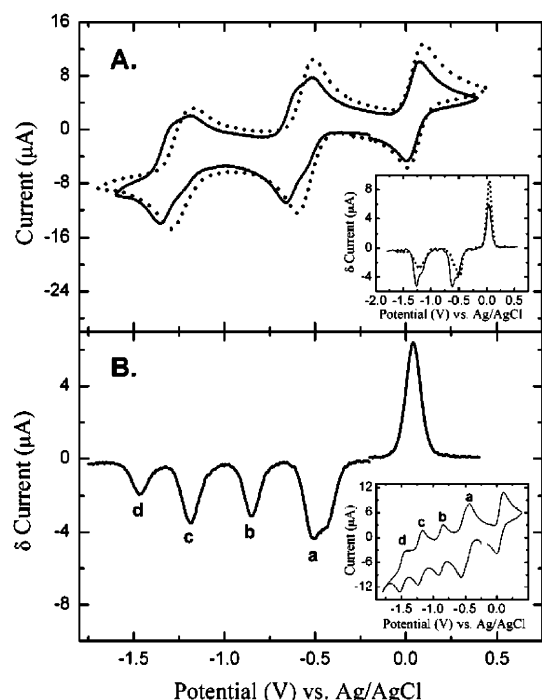


Figure 2. (A) CV of 2/dMeFc (···; 1.10/1.44 mM) and 3/dMeFc (—; 0.95/1.56 mM) under the same conditions as in Figure 1. (Inset): DPVs of 2/dMeFc (0.96/2.70 mM) and of 3/dMeFc (0.98/1.84 mM). (B) DPV of 4/dMeFc (0.87/1.02 mM). (Inset): Corresponding CV (0.1 V s⁻¹).

the first wave of **1** that $n_1 = 1.81 \pm 0.01$. Assuming that the diffusion coefficient of the first-wave reduction product is $0.7 \times D_1$, i.e., that the ratio of the diffusion coefficients of **1** and **1**^{(3-n₁)+} is equal to the ratio of the diffusion coefficients of BP and its 1-e reduced form,¹³ it is calculated from the second wave of **1** (Figure 1, inset B) that $n_1 = 1.84 \pm 0.06$. Thus, by DPV **1** uptakes an equal number of electrons in the first and second reductions.¹⁵ The voltammetric values of n_1 (~ 2) probably reflect the average orientation of **1** approaching the electrode and signify that e-hopping across the perimeter does not occur to a significant extent within this time frame. In this regard, **1** is a rigid system, and the distance between the pyridinium nitrogens is fixed at ~ 2 nm (by modeling). Since the rate of through-space e-transfer decreases exponentially with distance (attenuation factor = 10 nm^{-1}), the e-exchange rate between the BP centers in **1** would be $\sim 10^9$ times slower than the rate in contact either in solution or via branch flexibility.⁸

Figure 2 summarizes the redox chemistry of **2–4**. The overlapping waves of Figure 2A imply that both external and internal redox centers of **2** and **3** are accessible.¹⁶ Bulk electrolysis of **3** at -0.95 V vs Ag/AgCl affords $n_3 = 5.9 \pm 0.1$. To determine how many redox centers within a branch are accessible within a voltammetric time scale, it was necessary to resolve two redox waves, one assigned unambiguously to an external and one to an internal redox center. In that regard, the $-\text{NO}_2$ group of **4** is reduced between the two BP-based reductions (wave b, Figure 2B), and while the first reduction waves of the external and internal pyridinium groups overlap (wave a, Figure 2B), upon further reduction the $-\text{NO}_2$ group turns from a good electron acceptor ($\sigma_{p-\text{NO}_2} = 0.78$) to an extremely strong electron donor ($\sigma_{p-\text{NO}_2^-} = -0.97$),⁹ pushing negative the reduction wave of the “external” carbonyl group of **4** (wave d). Thus, the carbonyl-based reductions of the internal (wave c) and external (wave d) redox centers are resolved. Using $D_4 = 9.24 \pm 0.01 \times 10^{-6} \text{ cm}^2 \text{ s}^{-1}$ (by HPLC) as an approximation of the true D_i 's of the intermediate reduced forms,^{14a} it is calculated from the DPV of Figure 2B that $n_{4\text{-external}} = 1.38 \pm 0.06$ (from wave

b) and that $n_{4\text{-internal}} = 1.46 \pm 0.06$ (from wave c). Thus, the number of accessible redox centers within the branches is about equal to the number of accessible redox centers across the perimeter. Given the large separation between the external and internal BP groups (~ 1.6 nm from C=O to C=O), through-bond e-transfer is expected to be slow. Tunneling through the branches must be also ruled out.⁸ Electron hopping from the perimeter to the center is thermodynamically unfavorable as reduced external redox centers ($-\text{NO}_2$ and pyridinium) do not have the power to reduce the internal carbonyl. On the other hand, the $-(\text{CH}_2)_6-$ spacers along the branches may coil up, bringing the internal redox centers closer to the perimeter. This hypothesis is supported by the UV spectrum of the core, which is independent of the concentration but is affected by the substituents along the perimeter. Thus, the λ_{max} values of **1** and **3** are at 334 and 324 nm, respectively, corresponding to a stabilization by $2.1 \text{ kcal mol}^{-1}$, which is consistent with $\pi-\pi$ interactions between the external BP groups and the core.¹⁷ In summary, the rigidity of **1** provides a complementary view of the fact that fast e-transfer along the perimeter of core-branch systems requires flexible branches.⁸ From a practical viewpoint, redox equivalents emerging from the core of a rigid light-harvesting system would be localized at the tips of the branches they emerge from, creating issues of efficient bimolecular e-transfer to redox quenchers in their immediate environment. Flexible branches may not only facilitate e-transfer along the perimeter but may also fold, rendering internal redox centers more accessible.

Acknowledgment. We thank the NASA Glenn Research Center Director's Discretionary Fund (DDF) for financial support.

Supporting Information Available: Experimental Section. This material is available free of charge via the Internet at <http://pubs.acs.org>

References

- (1) Grayson, S. M.; Fréchet, J. M. *Chem. Rev.* **2001**, *101*, 3819–3867.
- (2) (a) Cameron, C. S.; Gorman, C. B. *Adv. Funct. Mater.* **2002**, *12*, 17–20. (b) Toba, R.; Quintela, J. M.; Peinador, C.; Román, E.; Kaifer, A. E. *Chem. Commun.* **2001**, 857–858.
- (3) Ceroni, P.; Vicinelli, V.; Maestri, M.; Balzani, V.; Müller, W. M.; Müller, U.; Hahn, U.; Oswald, F.; Vögtle, F. *New J. Chem.* **2001**, *25*, 989–993.
- (4) Ong, W.; Kaifer, A. E. *J. Am. Chem. Soc.* **2002**, *124*, 9358–9359.
- (5) Christensen, C. A.; Goldenberg, I. M.; Bryce, M. R.; Becher, J. *Chem. Commun.* **1998**, 509–510.
- (6) Ghaddov, T. H.; Wishart, J. E.; Kirby, J. P.; Whitesell, J. K.; Fox, M. A. *J. Am. Chem. Soc.* **2001**, *123*, 12832–12836.
- (7) Baker, W. S.; Lemon, B. L., III; Crooks, R. M. *J. Phys. Chem. B* **2001**, *105*, 8885–8894.
- (8) (a) Amatore, C.; Bouret, Y.; Maisonnaute, E.; Abruña, H. D.; Goldsmith, J. I. C. *R. Chimie* **2003**, *6*, 99–115. (b) Amatore, C.; Bouret, Y.; Maisonnaute, E.; Goldsmith, J. I.; Abruña, H. D. *Chem. Eur. J.* **2001**, *7*, 2206–2226.
- (9) (a) Leventis, N.; Zhang, G.; Rawashdeh, A.-M. M.; Sotiriou-Leventis, C. *Electrochim. Acta* **2003**, *48*, 2799–2806. (b) Leventis, N.; Rawashdeh, A.-M. M.; Zhang, G.; Elder, I. A.; Sotiriou-Leventis, C. *J. Org. Chem.* **2002**, *67*, 7501–7510.
- (10) Leventis, N.; Oh, W.-S.; Gao, X.; Rawashdeh, A.-M. M. *Anal. Chem.* **2003**, *75*, 4996–5005.
- (11) The peak-current potential separations (ΔE_{p-p}) are 68 ± 5 , 78 ± 5 , and 70 ± 5 mV for the first- and second-reduction waves of BP and for the dMeFc wave, respectively.
- (12) Bard, A. J.; Faulkner, L. R. *Electrochemical Methods, Fundamentals and Applications*, 2nd ed; John Wiley and Sons: New York, 2001.
- (13) Experimentally, the second redox wave of 4-benzoyl-N-methylpyridinium cation is $0.85 \times$ the first one.¹⁴ Looking up that ratio in Table 3 of ref 14a, it is deduced that the diffusion coefficient of the 1-e reduced form is $\sim 0.7 \times$ the diffusion coefficient of the parent species.
- (14) (a) Leventis, N.; Gao, X. *J. Phys. Chem. B* **1999**, *103*, 5832–5840. (b) Leventis, N.; Gao, X. *J. Electroanal. Chem.* **2001**, *500*, 78–94.
- (15) A similar analysis for the reduction of the carbonyl groups in the free base of **1** (1-FB) (dotted line in Figure 1, inset B) yields $n_{1\text{-FB}} = 1.66 \pm 0.02$. ($D_{1\text{-FB}} = 1.20 \pm 0.02 \times 10^{-5} \text{ cm}^2 \text{ s}^{-1}$ by HPLC.)
- (16) For the two waves of **2**, $\Delta E_{p-p} = 95 \pm 3$ mV and 114 ± 5 mV, respectively. Thus, their composite nature had to be confirmed by DPV: Figure 2A, inset.
- (17) For comparison, the $\pi-\pi$ interaction energy in methylene blue, as reflected in the absorption spectrum, is $\sim 4 \text{ kcal mol}^{-1}$. For example, see: Rabinowitch, E.; Epstein, L. F. *J. Am. Chem. Soc.* **1941**, *63*, 69–78.

JA0390247